Dynamical spin chirality and spin anisotropy in $Sr_{14}Cu_{24}O_{41}$: A neutron polarization analysis study

J. E. Lorenzo
Laboratoire de Cristallographie, CNRS, BP 166, 38042 Grenoble Cedex 09, France

C. Boullier and L. P. Regnault
Commissariat à l'Energie Atomique, Département de Recherche Fondamentale sur la Matière Condensée, SPSMS/MDN, 38054 Grenoble Cedex 9, France

U. Ammerahl
2. Physikalisches Institut, Universität zu Köln, D-50937 Köln, Germany

A. Revcolevschi
Laboratoire de Physico-Chimie des Solides, Université Paris-Sud-11, 91405 Orsay Cedex, France
(Received 22 June 2006; revised manuscript received 11 December 2006; published 22 February 2007)

Low-dimensional quantum spin systems constitute an ideal built-in laboratory to study fundamental aspects of solid-state physics. By engineering suitable compounds, fundamental theories have been tested during the past decades and many studies are still underway. Quantum phase transitions, possible coupling mechanisms to explain high-T_C superconductivity, ring exchange and orbital and spin currents, and the occurrence of Luttinger liquids and Bose-Einstein condensation are among the matters studied in this fascinating area of quantum systems. Here we add two values to this extensive list, which are the study of the spin anisotropy in spin-singlet ground-state compounds and the study of magnetic chirality, as measured by inelastic polarized neutron scattering techniques. To this end we have used the paramagnetic spin-singlet ground-state compound $Sr_{14}Cu_{24}O_{41}$ and discussed in detail the scattering properties of the first excited state of the chain sublattice, a spin triplet. In-plane and out-of-plane magnetic fluctuations are measured to be anisotropic and further discussed in the light of the current hypothesis of spin-orbit coupling. We show that under appropriate conditions of magnetic field and neutron polarization, the *trivial* magnetic chirality selects only one of the Zeeman-split triplet states for scattering and erases the other one that possesses opposite helicity. Our analysis pertains to previous studies of dynamical magnetic chirality and chiral critical exponents, where the ground state is chiral itself, the so-called *nontrivial* dynamical magnetic chirality. As it turns out, both trivial and nontrivial dynamical magnetic chiralities have identical selection rules for inelastic polarized neutron scattering experiments and it is not at all evident that they can be distinguished in a paramagnetic compound.

DOI: 10.1103/PhysRevB.75.054418 PACS number(s): 75.25.+z, 78.70.Nx, 74.72.−h

I. INTRODUCTION

Structural chirality is time-reversal even and parity-reversal odd, $PT=-+$ (or also called P asymmetry), whereas magnetic chirality breaks the invariance of both time and parity, $PT=--$ (or PT asymmetry). The importance of spin chirality in accounting for a certain number of properties has been set forth in the context of, for instance, strongly correlated electron systems.[1–4] Chiral spin fluctuations have been speculated to play a central role in establishing the normal-state properties in doped planar cuprates.[4] The presence of translation symmetry preserving[5] (or breaking[6]) *chiral* electron currents around the CuO_2 plaquettes has been invoked as a possible candidate for the superconducting order parameter of the high-T_C cuprates. This theory has received the support of dichroic studies of the photoemission signal[7] and, very recently, of neutron polarization studies.[8] In a combined work of transport measurement, neutron scattering, and theoretical calculation, Taguchi *et al.*[2] have evidenced that the gigantic anomalous Hall effect observed in the pyrochlore ferromagnet with geometrically frustrated lattice structure, $Nd_2Mo_2O_7$, is mostly due to the spin chirality. Finally, Hall resistivity $\rho(xy)$ and the magnetization M experiments of a canonical spin glass AuFe show that the difference between zero-field-cooled (ZFC) and FC measurements[3] is consistent with the predictions of the chirality scenario of canonical spin glasses by Kawamura.[9]

Under general grounds, magnetic inelastic excitations[10,11] are described as spin precessions around the quantization axis or, in the case of paramagnets, the magnetic field and the intrinsic spin chirality of the magnetic excitations of a collinear ferromagnetic structure can be revealed under appropriate experimental conditions. A strong enough external magnetic field favors magnetic domains of the appropriate direction and induces macroscopic T asymmetry.[12] Therefore, magnetic excitations have a built-in P violation regardless of whether or not the underlying magnetic structure violates P symmetry. This is what we shall call *trivial*[13] dynamic magnetochirality.

The question of how magnetic chirality appears in neutron scattering experiments has been theoretically tackled since the beginning of this technique.[14,15] The elastic case—spiral magnetic arrangements—has been widely studied in polarized neutron scattering experiments and the formalism can be checked in neutron scattering textbooks.[16,17] The possibility of the observation of the *nontrivial* magnetic order by

neutron scattering experiments, tensorlike multipolar orderings, was first formulated by Barzykin and Gor'kov[18] and later developed by Maleyev and co-workers[19–22] and applied to chiral compounds where chirality clearly arises from magnetic frustration.

Trivial[13] dynamic magnetochirality has been observed in the magnetic excitations of ferromagnetic compounds. Very recently, experimental evidence for chirality in the one-dimensional (1D) $S=1/2$ quantum Ising antiferromagnet $CsCoBr_3$ has been detected.[23] Excitations correspond to the flipping of a single spin, thus creating a domain wall and the propagation of two solitons in both directions of the chain. This type of dynamic magnetochirality[24] has been predicted by theory[25] and boldly deduced in unpolarized neutron scattering experiments under magnetic field.[26]

Recently, the quest for magnetic fluctuations issued from a chiral spin arrangement has raised a lot of interest. Following Kawamura's conjecture,[9] the magnetic phase transitions of *chiral* magnetic compounds should belong to a new universality class (the chirality universality class), with its own order parameters and novel critical exponents. Plakhty's group has conducted inelastic neutron scattering experiments on some well-known chiral compounds [in the triangular lattice antiferromagnets $CsMnBr_3$ and $CsNiCl_3$ (Refs. 27–29) and in the helimagnetic phase of Ho (Ref. 29)]. From the difference between the neutron counts for $\uparrow$ and $\downarrow$ neutron channels at nonzero energy transferred they claimed to have shown the presence of *dynamic* spin chirality and associated critical exponents above T_N (in the paramagnetic phase). In a parallel work, Roessli and co-workers[30] have shown the presence of dynamic spin chirality in the single-handed spiral ferromagnet MnSi. The critical exponent $\nu \approx 0.67$ (Refs. 30 and 31) is rather close to the value expected for chiral symmetry.[9] We define nontrivial magnetic dynamical chirality as that $PT=--$ component of the excitations arising from an antisymmetric vector arrangement $\mathbf{C}=\mathbf{S}_i \times \mathbf{S}_j$ or from electron spin currents that may be present in the compound.

Both trivial and nontrivial magnetic dynamical chirality neutron scattering cross sections share analogous selection rules, the former being more stringent than the latter. From experiments carried out on these systems it is far from obvious how one can actually separate both contributions. In this paper we address the issue of the measurement of *trivial* dynamic magnetochirality. The choice of the compound $Sr_{14}Cu_{24}O_{41}$ is not without purpose: it represents a suitable example of a two interpenetrating, noninteracting spin-liquid compounds where quantum spin fluctuations are seen to survive up to room temperature. We thereby present a detailed inelastic polarized neutron scattering study of the excitations in the paramagnetic compound $Sr_{14}Cu_{24}O_{41}$. This family of compounds exhibits a composite structure made up of a sublattice of $S=1/2$ spin chains and a sublattice of $S=1/2$ spin ladders. The magnetic excitations of the chain sublattice will be addressed here, with a special emphasis in (a) the anisotropy of the spin excitations of a degenerate spin triplet and (b) a thorough study of the spin-spin antisymmetric correlation functions. In view of the close relation between the observed anisotropy of the magnetic excitations and the occurrence of a nontrivial magnetic chirality we have decided to study both in this paper.

This paper is structured as follows: We first discuss the experimental details and the basic features of longitudinal neutron polarization analysis needed to follow the results of this paper. Next, the anisotropy of the magnetic excitations is characterized in two different experiments (i) by measuring the intensity of the spin-triplet components under magnetic field and (ii) by performing a neutron polarization analysis and extracting the spin-spin correlation functions in and out of the scattering plane. Polarization studies of the spin excitations under magnetic field, $H \| \mathbf{Q}$, allow measuring the influence of the antisymmetric spin-spin correlation (or *trivial chirality*) onto the scattering cross section. Finally, we speculate on the possible origin of the anisotropy of the spin-triplet correlation functions and on the impact of our studies on the observation of possible dynamic chirality features (or *nontrivial chirality*) in a neutron scattering experiment.

II. EXPERIMENTAL DETAILS

A. Longitudinal polarization analysis

Longitudinal polarization analysis[32] (LPA) has been largely used to study magnetic excitations in condensed matter. It consists of creating a spin-polarized incident neutron beam (the polarization rate of the incident beam is $\mathbf{P}_0$) along a given direction and measuring the number of neutrons scattered in the same direction and in the different polarization states, parallel or antiparallel with respect to the incident neutron polarization settings. If each of the polarization states is labeled by the direction of the neutron spin, + (or $\uparrow$) and − (or $\downarrow$), then the different cross sections are denoted by the pairs (++) and (−−) for the *non-spin-flip* (NSF) processes and (+−) and (−+) for the *spin-flip* (SF) ones. It can be easily shown that the most suitable reference system for the neutron polarization analysis refers to the scattering vector $\mathbf{Q}$, and thus we define the components as $x \| \mathbf{Q}$, $y \perp \mathbf{Q}$ and z vertical to the scattering plane. This method allows the determination of both nuclear and magnetic contributions by measuring the polarization cross sections for the three different directions of $\mathbf{P}_0$. Theoretical equations describing the cross sections and final polarization state have been independently derived by Blume[14] and Maleyev *et al.*[15] These equations and, in general, the LPA methodology have been recently revisited by us.[33] In what follows only the final equations will be given for the ideal case where polarizers and flippers behave as perfect devices:

$$\sigma_x^{\pm\pm} \propto N,$$

$$\sigma_x^{\pm\mp} \propto M_y + M_z \mp M_{ch},$$

$$\sigma_y^{\pm\pm} \propto N + M_y \pm R_y,$$

$$\sigma_y^{\pm\mp} \propto M_z,$$

$$\sigma_z^{\pm\pm} \propto N + M_z \pm R_z,$$

$$\sigma_z^{\pm\mp} \propto M_y, \tag{1}$$

where $\sigma_\alpha^{\beta,\gamma}$ is the short form of $(d^2\sigma/d\Omega d\omega)^{\beta,\gamma}(P_0 \| \alpha)$. For completeness, the unpolarized neutron scattering cross sec-

tion is $\sigma=N+M_y+M_z$. The notations of the above equations are as follows:

$$N=\langle N_Q N_Q^\dagger\rangle_\omega,$$

$$M_y=\langle M_{Qy}M_{Qy}^\dagger\rangle_\omega,$$

$$M_z=\langle M_{Qz}M_{Qz}^\dagger\rangle_\omega,$$

$$M_{ch}=i(\langle M_{Qy}M_{Qz}^\dagger\rangle_\omega-\langle M_{Qz}M_{Qy}^\dagger\rangle_\omega),$$

$$R_y=\langle N_Q M_{Qy}^\dagger\rangle_\omega+\langle M_{Qy}N_Q^\dagger\rangle_\omega,$$

$$R_z=\langle N_Q M_{Qz}^\dagger\rangle_\omega+\langle M_{Qz}N_Q^\dagger\rangle_\omega, \quad (2)$$

where $\langle N_Q N_Q^\dagger\rangle_\omega$ and $\langle M_{Q\alpha}M_{Q\alpha}^\dagger\rangle_\omega$ ($\alpha=y,z$) are the space and time Fourier transforms of the nuclear-nuclear and spin-spin correlation functions, respectively. R_y and R_z are the symmetric part of the nuclear-magnetic interference terms, and M_{ch} is the chiral (or antisymmetric) correlation function. It is worth noting that the antisymmetric part of the interference terms and the symmetric counterpart of the chiral correlation function are not accessible by the LPA technique as the polarization of the incident neutrons results rotated after scattering by these terms. In order to access these correlation functions the use of spherical neutron polarimetry based on, e.g., "Cryopad" devices[34,33] is mandatory.

Before closing this section on the LPA technique it is worth recalling that the last three correlation functions (M_{ch}, R_y, and R_z), if non-null, generate a polarized beam, when the incoming beam is unpolarized, $P_0=0$. The resulting polarization of the scattered neutrons is along x, y, and z directions, respectively, and the cross sections for this case are

$$\sigma_x^{0\pm}\propto N+M_y+M_z\pm M_{ch},$$

$$\sigma_y^{0\pm}\propto N+M_y+M_z\pm R_y,$$

$$\sigma_z^{0\pm}\propto N+M_y+M_z\pm R_z. \quad (3)$$

A variant of this last configuration has been used to select the chiral correlation function from the rest of symmetric contributions to the scattering cross section.[27–29] The alternative experimental situation consists of producing a polarized incoming beam and no polarization analysis is carried out in the scattered beam. Note that because of the symmetry of the equations, the very same terms can generate an unpolarized scattered beam out of a polarized incident one: $M_{ch}\equiv\frac{1}{2}(\sigma_x^{-0}-\sigma_x^{+0})\equiv\frac{1}{2}(\sigma_x^{0-}-\sigma_x^{0+})$. Finally, one has to keep in mind that the development of the neutron scattering cross sections is completely general and exclusively based on the properties of the magnetic interaction vector and neutron spin polarization. These equations are independent of the choice of a particular magnetic interaction (such as, for instance, the Dzyalozhinskii-Moriya antisymmetric spin exchange) or spin model.

B. Sample description and experimental conditions

Polarized neutron experiments were performed on the paramagnetic, spin-singlet ground-state compound

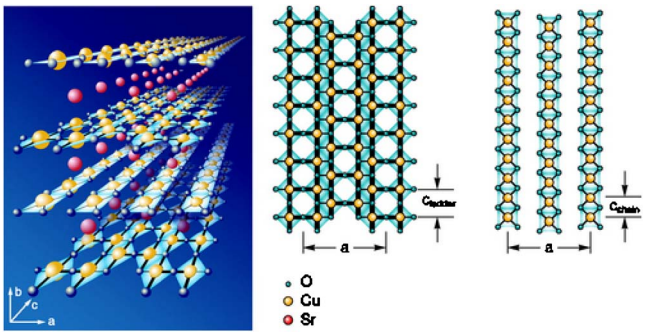

FIG. 1. (Color online) (Left) Structure of $Sr_{14}Cu_{24}O_{41}$. It consists of a stacking of layers of chains and layers of ladders separated by Sr (or Ca,La,….). (Right) Detail of the structure of the chain sublattice and the ladder sublattice.

$Sr_{14}Cu_{24}O_{41}$. This compound displays a composite structure made up of the stacking of two distinct low-dimensional Cu-O arrangements exhibiting a spin-singlet ground state.[35] The first subsystem is a one-dimensional lattice of edge sharing CuO_2 chains, and the second one is a 2D system of two-leg ladders, Cu_2O_3, the stacking direction being the b axis. Lattice parameters for the chain sublattice are $a=11.53$ Å, $b=13.37$ Å, and $c_l=3.93$ Å. The admixture of both subsystems originates a superstructure with a nearly commensurate ratio of chain and ladder units along the c direction, $10c_c\approx 7c_l$, which results in a rather large lattice parameter $c=27.52$ Å for the supercell. A representation of both atomic positions and magnetic system of chains and ladders is given in Fig. 1. As first reported by McCarron *et al.*[36] and later refined within the superspace formalism by Frost-Jensen *et al.*,[37] the CuO_2 sublattice is described in the *Amma* space group while the $SrCu_2O_3$ sublattice can be described in space group *Fmmm*. In between these two types of copper oxide layers, the layers of Sr atoms are interleaved and a number of dopings have been studied.[35] $A_{14}Cu_{24}O_{41}$ (A=Sr,Ca,La,…) is the only known spin-ladder material supporting carrier doping. Interestingly, by substituting Sr^{2+} by La^{3+} the number of holes in the unit greatly diminishes whereas Ca^{2+} doping favors a transit of holes from the chain sublattice to the ladder sublattice. Note that on going from pure Sr to pure Ca the b-lattice parameter shrinks by 1 Å and, for $x\approx 13.6$, superconductivity develops under pressure (3–5 kbar).[38,39]

In this paper, we have studied the chain subsystem. According to previous studies[40–42] the inelastic spectrum of the chain system has been investigated and a well-defined magnetic gap is observed around 11 meV for temperatures below $T<\Delta/k_B$. As there are two symmetry-different, hardly interacting chains per unit cell along a, two distinct triplet states appear (Fig. 2). To deal with the difficulty of separating well the two excited states, the experiment was carried out at $\mathbf{Q}=(-2.5,0,0.25)$ (and symmetry-related positions) where dispersion curves of the two distinct triplet states cross and a single mode appears at this position. As can be seen in Fig. 3, the magnetic ground state observed at low temperatures results from the peculiar charge ordering (hole ordering) developing in this compound where the extra holes serve to form Zhang-Rice singlets[40,43] at given Cu positions. Indeed, this

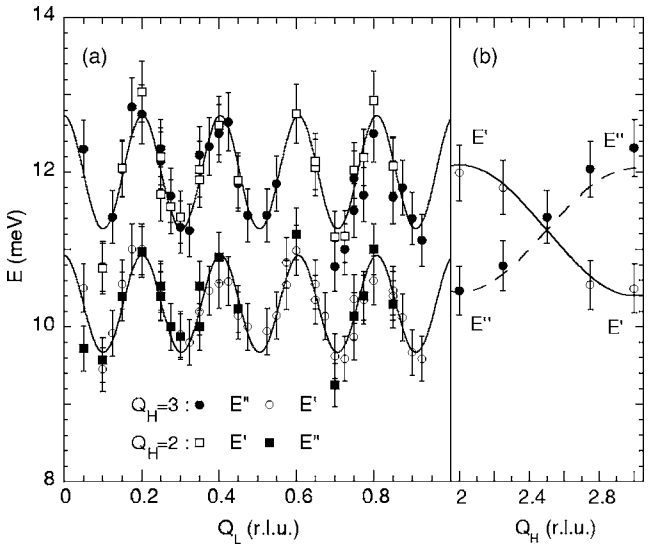

FIG. 2. Dispersion of the chain excitations along the *a* and *c* directions. The two parallel dispersion curves arise from the presence of two nonequivalent chains in the unit cell. The solid line is the result of a fit based on a isolated dimer model (Ref. 41) Experiments reported here have been carried out at $\mathbf{Q}=(-2.5,0,0.25)$, where the two branches merge and become degenerate.

charge ordering develops continuously *without* a real symmetry breaking phase transition and its origin still defies understanding. Remarkably, the refinement of the inelastic neutron scattering data has yielded a unique solution for the location of the magnetic moments and, from there, the determination of the charge order pattern.[41,42] This is in striking contrast with conventional x-ray and neutron diffraction studies that require the refinement of the intensities of the peaks from both the ladders and the chain sublattices, as well as of the interference peaks between both substructures. This extraordinary complexity hinders the realization of reliable crystallographic refinements,[44,45] and the whole issue is still under debate.[46] Therefore the study of the magnetic excitations, where both sublattices have different energy ranges with hardly no magnetic interference between them, offers the possibility of carrying out a sort of *unconventional* crystallography of the charges themselves, a matter that is otherwise challenging. The neutron scattering data on the pure $Sr_{14}Cu_{24}O_{41}$ agrees with the picture of 6-holes per chain per unit cell and hole-empty ladder sublattice. Recently, Abbamonte *et al.* have evidenced the presence of a hole crystallization in the ladder sublattice due to long-range Coulomb repulsion and without lattice distortion.[47,48] This feature, first revealed in the pure compound through the presence of a $5c_l$ ordering wave vector, has been further detected in the Ca-doped $Sr_3Ca_{11}Cu_{24}O_{41}$ with a $3c_l$ modulation.[49] In view of these results it is certain that the model used to analyze the q−dependence of the inelastic neutron scattering data and thus to locate the holes in the chain sublattice[40–42] needs to be revisited. However it does not cast any doubt that magnetic excitations are issued from spin-singlet to spin-triplet transitions and this feature will be utilized all through this paper.

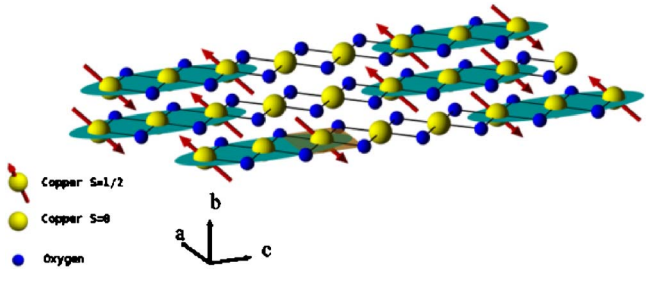

FIG. 3. (Color online) Hole ordering and the concomitant magnetic arrangement in the chain sublattice as has been determined at low temperatures by inelastic neutron scattering experiments (Ref. 41). The green shadowed area represents the spatial extension of the spin dimer, where spin-spin superexchange takes place through a $S=0$ Zhang-Rice singlet at the Cu.

Our $Sr_{14}Cu_{24}O_{41}$ sample was cut from an ingot grown by the travelling-solvent zone method under a pressure of 3 bars of oxygen.[50] The sample used in the inelastic neutron scattering experiment is made up of a set of five cylindrically shaped single crystals of volume $5\times5\times10$ mm^3 with the *c*-axis along the rod with a misalignment among the five single crystals of the order of ±0.5°.

Experiments were carried out on the CRG three-axis spectrometer IN22 at the Institut Laue-Langevin, set in three different monochromator-analyzer configurations: (i) pyrolitic graphite- (PG-) PG, for standard unpolarized studies, (ii) Heusler-Heusler, for full polarization analysis studies, and (iii) PG-Heusler, for experiments where only the polarization of the scattered beam is analyzed, out of a unpolarized incoming beam, and three different sample environment configurations: (i) ILL-type orange cryostat, available to cover the range 1.4–300 K, (ii) vertical superconducting magnet of 12 T (for the polarized neutron scattering experiments, a 6-T superconducting magnet was used and the maximum polarizing field was 3 T) and (iii) horizontal superconducting magnet of 4 T.

Figure 4 shows a sketch of the experiment. Particular care has been taken to determine the flipping ratio for the different field configurations. In order to minimize the effect of the variation of the cryomagnet stray fields during the course of the scans, the flipper currents (between 6 and 9 A to yield a field of the order of 70 G) were tuned to operate at 3π flipping, instead of the most classical π flipping. This operation mode has required the development of a special water-cooled flipper as the current for the 3π flipping is 3 times larger than that of the π flipping. Ideally, one would like to run the flipper at higher flipping angles. However, this implies a concommitant increase of the current in the flippers that gives rise to an augmentation of the thermal charge, difficult to dissipate in such compact devices. In the 3π-flipping mode, a flipping ratio as high as $\rho_F=30$ was achieved at 2.662 Å^{-1}.

Inelastic scans were performed at fixed final wave vector $\mathbf{k}_f=2.662$ or 3.84 Å^{-1}, and a 40-mm-thick graphite filter was used after the sample to minimize higher-order flux contamination. The neutron measurements were performed with the $(\mathbf{a},\mathbf{c})$ crystallographic plane parallel to the scattering plane. The magnetic field was applied either vertical to the scattering plane (parallel to the *b* axis) or parallel to the scattering vector. Only the chain-sublattice magnetic excitations are

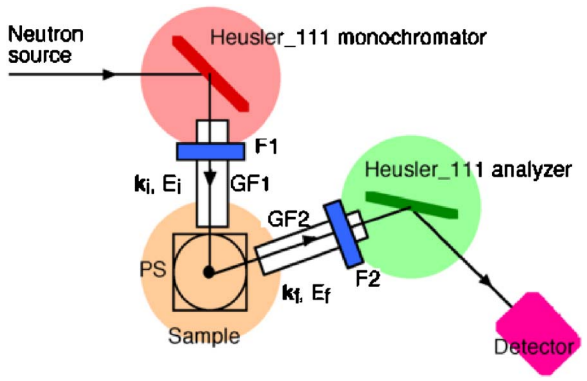

FIG. 4. (Color online) Sketch of the experimental device for the type-2 configuration. Neutrons were monochromatized and vertically polarized by means of a Heusler crystal—say, in the + state; by creating a magnetic field of ≈70 G the flipper (F1) allows for a $+\rightarrow-$ neutron *flip* if required. After being conducted and preserved from depolarization by a guide field (GF1), neutrons are aligned along a given polarization direction with the help of either modified Helmholtz four set coils (three coils horizontally spanning 120° each and one vertical) or a horizontal and vertical superconducting magnet. After interaction with the sample, neutrons follow through a guide field (GF2) and can be vertically flipped (F2) if required $(-\rightarrow+)$. Finally, a second Heusler crystal, having the same setting as the first one, selects the corresponding polarization channel and energy analyzed the neutrons.

here reported, and the experiments were performed in the energy transfer range 8–15 meV, with typical resolution of the order of 1.5 meV [full width at half maximum (FWHM)]. The ladder excitations appear to have a spin-singlet to spin-triplet gap of 31 meV, and an analogous study will be reported elsewhere.[51]

C. Description of the spin-triplet and correlation functions

The spin pairing takes place through a nonmagnetic Cu (Zhang-Rice singlet); the description of the spin excitations in terms of the lowest-lying energy levels suffices to account for the inelastic neutron scattering data (below 40 meV). Indeed a full description of the magnetic dimer unit involves electronic orbitals of not less than three CuO_2 units (see Fig. 3) which, in view of the large degrees of freedom involved, may result in a large number of excited states. Despite the apparent complexity of the spin chain sublattice ground state, the theoretical framework to account for the lowest-lying excited states is rather trivial. It is certain that, at some point in the analysis, a full description of the electronic states and their hybridizations ought to be invoked. This is particularly true if one wants to explain the anisotropy of the spin susceptibility.[52]

At sufficiently low temperatures $T<\Delta/k_B$, the paramagnetic excitations become very well defined and the recorded spectra are energy resolution limited. Spin-singlet–to–triplet transitions can be evaluated by using the equation

TABLE I. Value of $\langle \mathbf{0}|\hat{\mathbf{S}}|\mathbf{1}\rangle$ for the different components of the triplet, **1**. These are labeled, following the notation $|Ss_z\rangle$.

	S_X	S_Y	S_Z
$\|10\rangle$	0	0	$\sqrt{2}$
$\|11\rangle$	1	$-i$	0
$\|1\bar{1}\rangle$	1	i	0

$$\frac{d^2\sigma}{d\Omega d\omega} = r_0^2 \frac{k'}{k} \sum_{\alpha\beta} (\delta_{\alpha\beta} - \tilde{k}_\alpha \tilde{k}_\beta) \sum_{v,v'} p_n \langle \Gamma_n v | \hat{Q}_\alpha^+ | \Gamma_n' v' \rangle \times \langle \Gamma_n' v' | \hat{Q}_\beta | \Gamma_n v \rangle, \quad (4)$$

and therefore the scattering cross section is proportional to $\langle \mathbf{0}|\hat{\mathbf{S}}|\mathbf{1}\rangle\langle \mathbf{1}|\hat{\mathbf{S}}|\mathbf{0}\rangle$, with $|\mathbf{0}\rangle \equiv |\mathbf{00}\rangle \equiv |\uparrow\downarrow\rangle - |\downarrow\uparrow\rangle$ the spin singlet and $|\mathbf{1}\rangle \equiv \{|\mathbf{11}\rangle, |\mathbf{10}\rangle, |\mathbf{1\bar{1}}\rangle\} \equiv \{|\uparrow\uparrow\rangle, |\uparrow\downarrow\rangle + |\downarrow\uparrow\rangle, |\downarrow\downarrow\rangle\}$, the spin triplet. By using the traditional axis for quantum mechanic calculations ($\sigma_X|\uparrow\rangle = |\downarrow\rangle$, $\sigma_Y|\uparrow\rangle = i|\downarrow\rangle$, and $\sigma_Z|\uparrow\rangle = |\uparrow\rangle$ and identically for $|\downarrow\rangle$) the scattering probabilities are found to be those in Table I.

III. RESULTS

A. Magnetic excitations without polarization analysis

The excitations corresponding to the spin chain sublattice have been studied in detail,[40–42] albeit without neutron polarization analysis. Under a field of 11.5 T, the resolution conditions are such that the three components of the Zeeman-split triplet can be well separated (see Fig. 5). From the peak positions $\hbar\omega_1 = \hbar\omega_0 - g_b\mu_B H_b = 9.8$ meV, $\hbar\omega_0 = 11.3$ meV, and $\hbar\omega_{\bar{1}} = \hbar\omega_0 + g_b\mu_B H_b = 12.8$ meV, the value of the Landé factor perpendicular to the chain axis can be calculated, $g_b = 2.31 \pm 0.06$, in agreement with magnetic susceptibility[53] and electron spin resonance (ESR)[53–55] data. No nuclear component has been detected at this **Q** position, and the scattering cross sections are $\sigma(Q, \hbar\omega_0 \pm g\mu_B H) + \sigma(Q, \hbar\omega_0)$. The direction of the magnetic field, z, imposes this direction to be the

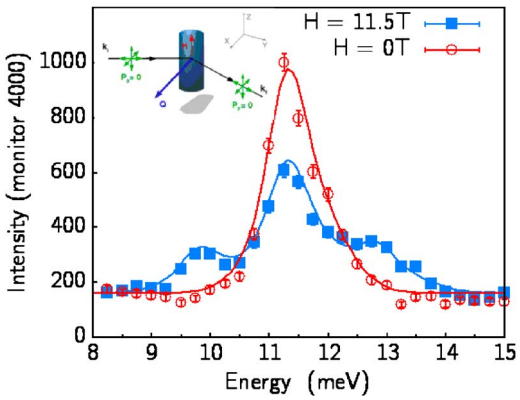

FIG. 5. (Color online) Unpolarized neutron scan of the Zeeman splitting of the triplet at $\mathbf{Q} = (-2.5, 0, 0.25)$ at $H = 11.5$ T (vertical), and comparison with $H = 0$. The neutron polarization conditions appear as an inset.

quantization axis which, from Table I, implies that $Z \equiv z$. Under these circumstances and by looking at the results in Table I one can safely conclude that $\sigma(Q, \hbar\omega_0 \pm g\mu_B H) \equiv M_y$ and $\sigma(Q, \hbar\omega_0) \equiv M_z$.

A careful analysis of the integrated intensities of the three peaks reveals that these are weaker than that of the degenerate $H=0$ T, integrated intensity, $I_{1,\bar{1}}(H=11.5\ \text{T}) = 0.35 I_0(H=0)$ for the side peaks and $I_0(H=11.5\ \text{T}) = 0.54 I_0(H=0)$ for the unshifted one. Therefore, the ratio $M_z/[M_y(\hbar\omega_{\bar{1}}) + M_y(\hbar\omega_1)]$ is not 1 but rather 1.54 ± 0.1, which leads to the conclusion that the magnetic fluctuations are anisotropic. These values of the intensities obtained under magnetic field, once added, yield the same amount as that obtained for the intensity of the degenerate triplet at $H=0$ T.

B. Magnetic excitations under polarization analysis

Polarized neutrons are most frequently utilized in experiments aimed at separating nuclear and magnetic contributions to the scattering. By inspecting the polarized neutron scattering equations [Eqs. (1)] one realizes that the configuration $P_0 \| \mathbf{Q}$, independently of the direction of the magnetic moments, is the most simple way to discriminate between both contributions. Indeed, the NSF cross sections ($\sigma_x^{\pm\pm}$) contain the nuclear contribution alone, whereas the SF channel ($\sigma_x^{\pm\mp}$) is proportional to the components of the magnetization perpendicular to $\mathbf{Q}$, $M_y + M_z \mp M_{ch}$. Results at $H=0$ T (Fig. 6) show that the NSF contribution is zero, and therefore a pure magnetic scattering appears at the $\mathbf{Q}$ position of the experiment. Before closing this section, it is important to recall that polarization analysis implies the presence of a rather small polarizing field at the sample position ($H_p \approx 0.1$ T) in order to prevent neutron depolarization. Therefore, and strictly speaking, the sample is never at $H=0$ T in our polarized neutron scattering experiments. The spin-triplet splitting introduced by this field is 10 times smaller than the energy resolution, and therefore the effect of H_p is irrelevant in our experiment.

1. Anisotropy in the vertical field configuration

As already mentioned above and shown in Fig. 5, inelastic neutron scattering experiments at rather high magnetic fields have revealed an unexpected anisotropy between the $|11\rangle$ (or $|1\bar{1}\rangle$) and $|10\rangle$ components of the spin-triplet or, in other words, between the in-plane (M_y) and out-of-plane (M_z) spin-spin correlation functions. An identical conclusion can be drawn from studies at zero field and under a polarized beam. Indeed, and in the absence of a nuclear contribution [N and R_z are zero in Eqs. (1)], the configuration $P_0 \| z \perp \mathbf{Q}$ readily implies that the signal in the NSF channels ($\sigma_z^{\pm\pm}$) is proportional to M_z whereas M_y correlation functions appear in the SF channels ($\sigma_z^{\pm\mp}$). Results are shown in Figs. 7 and 8 for $\mathbf{Q}=(-2.5\ 0\ 0.25)$. Note that the use of a magnetic field in this experiment is exclusively justified in terms of *cosmetic* reasons and does not bring relevant information other than to separate the $s_z=1$ from the $s_z=\bar{1}$ components of the triplet. Identical studies can be carried out at different $\mathbf{Q}$ positions, and data are displayed in Table II. Regardless of the $\mathbf{Q}$ position, an anisotropy in the susceptibility of the order of 30%, first evidenced in susceptibility measurements, is thus confirmed by our analysis of the spin-spin correlation functions. The fact that this ratio is roughly independent on Q_c implies that magnetic fluctuations within the (a,c) plane are isotropic. The origin and magnitude of this anisotropy is puzzling and difficult to justify in terms of the current, although simplified, models of spin-spin interactions. In the case of an S

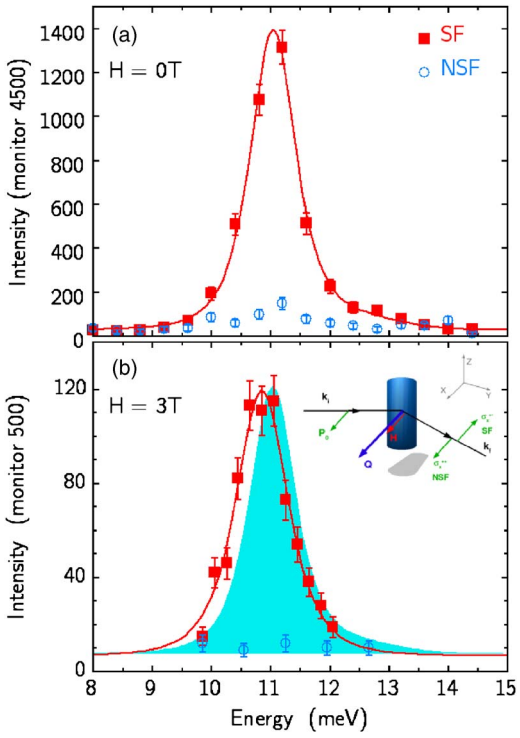

FIG. 6. (Color online) (a) Polarized ($P_0 \| \mathbf{Q}$) neutrons energy scan at $\mathbf{Q}=(-2.5, 0, 0.25)$ and with $H=0$ T. The scattering cross sections are σ_x^{--} in blue and σ_x^{-+} in red. The fact that $\sigma_x^{--} \approx 0$ (except for background correction) implies that the excitations measured at this $\mathbf{Q}$ position and energy are purely magnetic. (b) Same scan under horizontal magnetic field of 3 T with σ_x^{++} in blue and σ_x^{+-} in red. As for a comparison we have included the $H=0$ T data as a blue shadow. Data at $H=3$ T clearly display a shift to low energies whereas no signal appears at high energies.

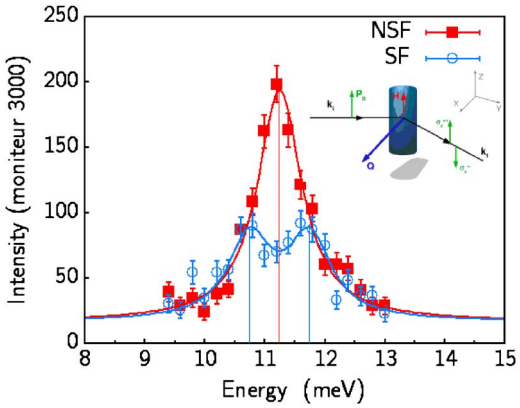

FIG. 7. (Color online) Polarized inelastic spectra under a vertical magnetic field of 4 T with σ_z^{++} in red and σ_z^{+-} in blue.

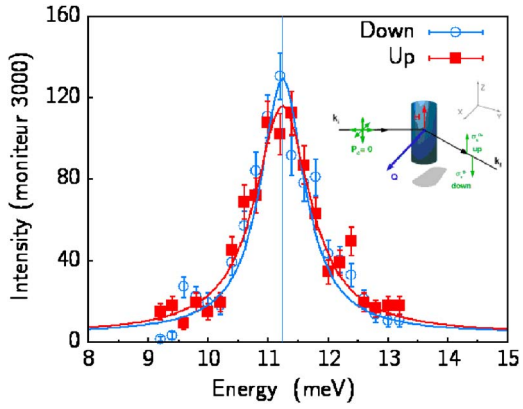

FIG. 8. (Color online) Inelastic spectra at $H=4$ T and with unpolarized incoming beam $P_0=0$ (Graphite-Heusler). Cross sections are σ_z^{0+} in blue and σ_z^{0-} in red.

$=1/2$ system, the single-ion anisotropy is zero. Other well-known sources of anisotropy are the Dzyalozhinskii-Moriya (DM) antisymmetric interactions. However, this antisymmetric interaction will in turn break the spin-triplet degeneracy and such a splitting has not been observed in our experiments. Moreover, the DM interaction is not allowed by symmetry in this compound. We shall come back to this point below.

2. Study of the magnetochiral correlation function

Magnetic excitations are defined as spin precessions around the quantization axis. In the absence of a magnetic field, energy minimization considerations dictate that there be an equal number of spins pointing up ($n_\uparrow$) and pointing down ($n_\downarrow$) (Ref. 56) and, therefore, there is no net macroscopic helicity in the excitations spectra. In a paramagnet the magnetic field defines the quantization axis which, in addition, defines the beam polarization direction. In this configuration $H\|\mathbf{Q}\|x$, the spin correlations that one have access to are M_y and M_z (symmetric) and M_{ch} (antisymmetric) [see Eqs. (1) and (2)]. We shall call this latter term *trivial* dynamical magnetochirality [proportional to the difference $(n_\uparrow - n_\downarrow)$] in order to distinguish it from the proposal of magnetochiral fluctuations issued from an odd-parity magnetic arrangement.[27–29] The necessary condition for its observation requires either a completely polarized neutron beam or at least that one of the components of the polarization (incoming or outgoing beam) be well defined. As has been pointed out in the Introduction, this condition, however, does not suffice to observe it as time reversal symmetry should be broken (macroscopically) in order to have only one of the helicities in the ground state or at least to unbalance them. Dynamical magnetochirality should be observed in uniaxial ferromagnets and ferrimagnets and paramagnets under an external magnetic field, either by creating a single domain (in the former) or by privileging a given direction (in the latter).

So far we have discussed the paramagnetic state of compounds that are going to magnetically order as temperature is decreased. A different class of paramagnetic compounds is that of the compounds exhibiting a nonmagnetic spin-singlet ground state down to the lowest temperatures. Here magnetic fluctuations arise from the population of the first (and beyond) excited state, a $S=1$ spin triplet. Apart from the compound under consideration, 1D spin chains such as $CuGeO_3$,[57] NaV_2O_5,[58] the high-T_C superconductors, the frustrated dimer arrangement $SrCu_2(BO_3)_2$,[59] or the spin-ladder compounds CuHpCl,[60,61] $(VO)_2P_2O_7$,[62,63] etc., display a spin-singlet ground state. Paramagnetic excitations appear at the spin-triplet gap and above, and are clearly inelastic at sufficiently low temperatures.

The spin-spin correlation functions for the spin-singlet to spin-triplet transition can be easily calculated (see Table I). Here $|11\rangle$ and $|1\bar{1}\rangle$ excitations describe right- and left-handed helices, respectively. The experiment was carried out with a magnetic field of 3 T parallel to $\mathbf{Q}$, which imposes the quantization direction for the excitations and thus removes the degeneracy of the modes $(P\|\mathbf{Q}\|Z)$. Following the results given in the Appendix, one can immediately see the effect of the chiral term in each of the energy-shifted triplets: for the right-handed component $|11\rangle$, the mode appears at $\hbar\omega_1 = \hbar\omega_0 - g\mu_B H$ and the scattering cross section is $\sigma_x^{+-}(11) \propto M_{1,1} + M_{ch,1} + O(M_{ch,1}/\rho_F)$. For the left-handed component $|1\bar{1}\rangle$, the mode appears at $\hbar\omega_{\bar{1}}(1\bar{1}) = \hbar\omega_0 + g\mu_B H$. The chiral term enters the scattering cross section with the sign reversed which, in the absence of spin anisotropy, leads to a cancellation with the symmetric spin-spin correlation function and yields a nearly null scattering cross section except for terms inversely proportional to the flipping ratio, $\rho_F=30$. The scattering equation thus reads $\sigma_x^{+-}(1,\bar{1}) \propto M_{1,\bar{1}} - M_{ch,\bar{1}} \approx 0 + O(M_{ch,\bar{1}}/\rho_F)$. By reversing the direction of the magnetic

TABLE II. Measurement of the magnetic susceptibility anisotropy M_z/M_y of the chain sublattice at $T=2.5$ K and $H=0$ T.

Q	ω (meV)	M_z	M_y	Background	Monitor	Counting time (s)	M_z/M_y
(−2, 0, 0.3)	10	442	339	30	5000	2430	1.33±0.11
	11.3	334	270	30	5000	2519	1.28±0.15
(−2, 0, 0.7)	11	437	290	25	4000	2010	1.58±0.14
	11	127	101	38	4000	2018	1.29±0.27[a]
(−3, 0, 0.3)	10	470	348	44	8000	3998	1.60±0.15
	11.3	274	194	28	5000	2515	1.60±0.23
(−3, 0, 0.7)	10	598	477	50	5000	2422	1.22±0.12

[a]Temperature for this point was 150 K.

field with respect to **Q** or by reversing the neutron polarization directions or even by conducting the experiment at neutron energy gain [64] the $|1\bar{1}\rangle$ component can be materialized. Figure 6(b) shows the effect described above for the $\sigma_x^{+-}(11)$ scattering channel. As shown in the Appendix, if the anisotropy of the spin-spin correlation function is taken into account, then $\sigma_x^{+-}(1,\bar{1}) \neq 0$. However, for the values of the anisotropy found in the preceding section, the calculation shows that $\sigma_x^{+-}(1,\bar{1})$ amounts to 2.4% of $\sigma_x^{+-}(1,1)$ and, therefore, should barely show up above background.

This effect of the neutron beam polarization on the split triplet is even more spectacular when the incident beam is unpolarized and the final neutron polarization is analyzed, parallel and antiparallel to the applied magnetic field (and to **Q**). The corresponding scattering cross sections are now σ_x^{0+} and σ_x^{0-}, respectively. Under these conditions, the $|11\rangle$ component of the triplet appears in the + channel whereas the $|1\bar{1}\rangle$ appears in the − channel. This is just the consequence of having − and + polarized neutrons along x in the incident beam (neutrons polarized otherwise do not contribute to the measured cross section), respectively. Figure 9(a) shows that, for $H=0$ T, the scattered intensities are the same for both + and − channels and little can be said about the origin of the signals. When the horizontal magnetic field is applied [Fig. 9(b)] each one of the channels displays the effect predicted by theory.

The difference $\sigma_x^{0+} - \sigma_x^{0-}$ (Fig. 10) bears an astonishing resemblance to the result proposed as the signature of the dynamical chirality in some paramagnetic compounds,[27–29] but centered at 11.3 meV instead of at zero energy. Apart from the energy location, our figure is connected to the trivial chirality of the magnetic excitations whereas in theirs the authors have claimed that it is the signature of chiral magnetic fluctuations induced by a magnetically chiral ground state,[27–29]—i.e., the nontrivial magnetochiral fluctuations. Disclosed from the argument outlined above, the actual contribution to this difference is $I_{diff} \cong M_{1,1} + M_{ch,1} - (M_{1,\bar{1}} + M_{ch,\bar{1}}) + O(M_{ch,1}/\rho_F, M_{ch,\bar{1}}/\rho_F)$ which, in our conditions, reads as $|M_{1,1}| \cong |M_{ch,1}|$ and identically $|M_{1,\bar{1}}| \cong |M_{ch,1}|$. Therefore, I_{diff} is a proper measure of chirality. Note that we have included a different term of chirality for each one of the triplets as, in general, the nontrivial chirality may favor one or the other. In the absence of nontrivial magnetochirality both terms are identical, although centered at their respective magnetic-field Zeeman-split positions.[65]

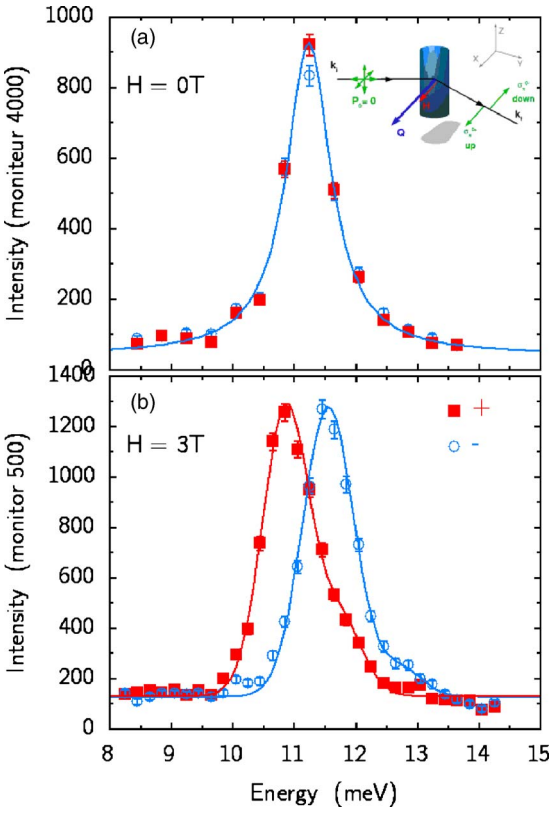

FIG. 9. (Color online) (a) Inelastic spectra at $H=0$ T and with unpolarized incoming beam $P_0=0$ (Graphite-Heusler). Cross sections are σ_x^{0+} in blue and σ_x^{0-} in red. In this case the + and − are related to the sign of **Q**. (b) The same with a horizontal magnetic field $H=3$ T oriented in the same direction as **Q**. In the presence of an applied magnetic field σ_x^{0+} measures the $|11\rangle$ component of the triplet whereas σ_x^{0-} measures the $|1\bar{1}\rangle$ component. Because of the selection rules for $P \| \mathbf{Q} \| M_Z$, $|10\rangle$ does not appear in the spectra.

IV. DISCUSSION

A. Magnetic anisotropies

Our polarized inelastic neutron scattering experiments have revealed an anisotropy between the magnetic fluctuations along a^*, c^* (or in the plane of the chains), and b^* (the stacking direction). First elastic neutron scattering results in antiferromagnetic La_2CuO_4 (Ref. 66) and $Sr_2CuO_2Cl_2$ (Ref. 67) have indicated deviations from the spherical spin density in the measured Cu form factor. It was later revealed that the experimental data could be well accounted for if the anisotropy of the symmetry of the orbital where the hole resides, $3d_{x^2-y^2}$, is taken into account.[68] Some *related* anisotropy has been found in other Cu^{2+} spin-singlet ground-state compounds such as $CuGeO_3$,[57] $BaCuSi_2O_6$,[69] and also the chain part of $Sr_{14}Cu_{24}O_{41}$.[53] It also appears in compounds where

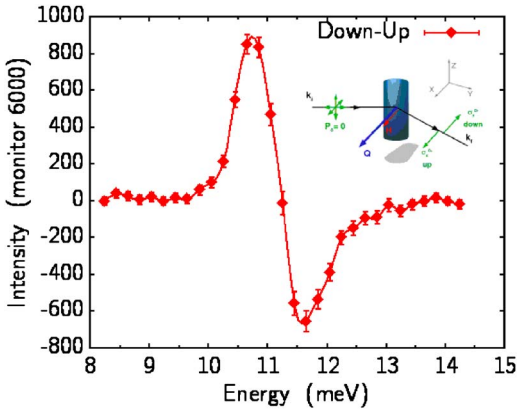

FIG. 10. (Color online) Difference $\sigma_x^{0+} - \sigma_x^{0-}$ for a horizontal magnetic field of 3 T ($\mathbf{Q} \| H$), following the data in Fig. 9(b). The solid line is a guide to the eye.

the absence of holes and the near-90° Cu-O bonding leads to the condensation of a ferromagnetic order along the chains and to an antiferromagnetic order among the chains. This is the case of Li_2CuO_2 (Refs. 70–72) and $La_5Ca_9Cu_{24}O_{41}$ (Ref. 73) in which the magnetic moments point along the stacking direction. Experiments under magnetic fields have shown a nearly Ising behavior [75] that underlines the rather strong anisotropy for this spin-1/2 compound. There is, in addition, a substantial magnetic moment at the oxygen sites, $0.1\mu_B$ for the former and $0.02\mu_B$ for the latter. The occurrence of a magnetic polarization of the oxygen sites gives experimental support to the rather strong covalency effects present in this compound. Whether or not it is a signature of some circulating currents (that involved no free electrons) as well, the origin of such anisotropy remains unclear yet.

It is well established that, in the absence of sizable spin-orbit coupling, the magnetic moment of Cu^{2+} would be isotropic and equal to $1\mu_B$ ($g=2$). The spin-orbit coupling introduces the mixing of the ground state with the excited states, yielding an orbital contribution to the wave function. This orbital contribution (a) modifies the magnetic moment and (b) introduces an anisotropy in the g values, $g_a \neq g_b \neq g_c$. Early ESR experiments on $Sr_{14}Cu_{24}O_{41}$ (Ref. 53) have revealed that the Landé tensor is anisotropic ($g_a=2.05$, $g_b=2.26$, and $g_c=2.04$) and temperature independent. The values for the anisotropy of the Landé factors are typical for a Cu ion in a square planar coordination of the oxygen ligands.

A second mechanism that renders anisotropy is the spin-orbit interaction associated with antisymmetric spin-(super)exchange interactions, or Dzyalozhinskii-Moriya interactions. In pure La_2CuO_4 the Dzyaloshinskii-Moriya antisymmetric exchange terms are generated by the small rotation of the CuO_6 octahedron, which creates the magnetic anisotropy in the CuO_2 plane as well as the canting of the Cu^{2+} moments out of the plane.[74] In this case the standard Heisenberg Hamiltonian

$$H[S] = J\vec{S}_1 \cdot \vec{S}_2 \tag{5}$$

transforms into

$$H[S] = \left(J - \frac{\vec{D}^2}{4J^2}\right)\vec{S}_1 \cdot \vec{S}_2 + \vec{D} \cdot (\vec{S}_1 \times \vec{S}_2) + \frac{1}{2J}(\vec{D} \cdot \vec{S}_1)(\vec{D} \cdot \vec{S}_2), \tag{6}$$

with $J=4t^2/U$ the antiferromagnetic superexchange and $\vec{D}=8t\vec{t}/U$ the Dzyalozhinskii-Moriya vector. t and $\vec{t}$ are the transfer integrals, $|\vec{D}| \propto |\vec{t}| \propto \lambda$, and λ is the spin-orbit coupling constant. The third term is an anisotropic exchange that is of second order in the spin-orbit coupling. It is this term that provides the anisotropy as $|\vec{D}|/J \propto \Delta g/g$. The caveat of this DM interaction is that it must result in a splitting of the triplet of excitations as is the case in the frustrated spin-dimer compound $SrCu_2(BO_3)_2$.[76] Notwithstanding, Shekt-mannn, Entin-Wolhman, and Aharony[77] (SEA) have realized that there is a hidden symmetry in the Hamiltonian above which can be written in the form

$$H[S'] = \left(J + \frac{D^2}{4J}\right)\vec{S}'_1 \cdot \vec{S}'_2, \tag{7}$$

with $S_1^{\pm\prime} = e^{\pm i\theta/2}S_1^{\pm}$, $S_1^{z\prime} = S_1^z$, $S_2^{\pm\prime} = e^{\mp i\theta/2}S_2^{\pm}$, and $S_2^{z\prime} = S_2^z$. This Hamiltonian, with this definition of the spins, is exactly isotropic and therefore has the same eigenvalues and eigenvectors as the previous one. The triplet remains degenerate and anisotropic as required by the experimental results. It was later pointed out that some restrictions apply to SEA's result in that the hidden degeneracy exclusively appears in the case of the one-band model and that the degeneracy is raised once the multiorbital aspect is taken into account.[78,79] Moreover, Hund's rule coupling was not considered in the SEA transformation which again will act so as to raise the degeneracy of the triplet. Finally, and despite the complexity related to the stacking of misfitted chain and ladders sublattices in the unit cell, both sublattices remain centrosymmetric down to low temperatures, thus preventing the onset of DM exchange interactions.

Magnetic anisotropies derived from anisotropic superexchange interactions have been found in the spin-wave spectrum in the magnetically ordered phase of antiferromagnetic cuprates. In this case, well-documented experiments[80] and theory[81,82] have evidenced an easy-plane anisotropy originating from a subtle interplay of spin-orbit and Coulomb exchange interactions. This result is very robust and has comparable magnitudes for many orthorhombic and tetragonal cuprates. A strong anisotropy of the superexchange in the 90° Cu-O chains has been advanced as a very likely property of the CuO_2-type chains,[83] thus underlining the importance of orbital degrees of freedom here, as well. This third possibility has been invoked to explain the very large linewidth of the ESR signal in $La_{14-x}Ca_xCu_{24}O_{41}$ (Refs. 54 and 55) and $LiCuVO_4$ (Ref. 84) and the inelastic neutron scattering data on the magnetic excitations in Li_2CuO_2 (Ref. 72) and $Ca_2Y_2Cu_5O_{10}$ (Refs. 85 and 86). ESR studies of pure $Sr_{14}Cu_{24}O_{41}$ (Ref. 55) have disclosed a similar anisotropy as well as a particular temperature dependence of the linewidth, constant up to $T^* \approx 200$ K and then linearly increasing. This temperature marks the onset of a 1D charge melting, and it does not correspond to a real phase transition. Similar drastic changes above T^* have been observed in the spin excitations of the chain sublattice[41,42] and in the temperature evolution of some Bragg reflections.[45,46] However, and contrary to what is expected, the broadening of the ESR line shape in $Sr_{14}Cu_{24}O_{41}$ amounts to 1/100 of that observed in $La_5Ca_9Cu_{24}O_{41}$, thus ruling out the influence of the anisotropic superexchange in $Sr_{14}Cu_{24}O_{41}$.

It seems that for this compound the presence of long-range-ordered Zhang-Rice hole pairs helps stabilize and strengthen the antiferromagnetic interactions (and, from that, the presence of a large spin gap for a Cu-O-Cu superexchange close to 90°); the exchange coupling becomes drastically different as now next-nearest-neighbor couplings have to be taken into account as well.[55] Thus the theoretical model casts describing all the above mentioned compounds[83] turn out to be inadequate for chain compounds having a rather strong antiferromagnetic Cu-Cu superexchange as is found in pure $Sr_{14}Cu_{24}O_{41}$. The case of superexchange, coupling me-

diated by a double bridge (see Fig. 3) has been recently considered[87] following embedded crystal fragment, *ab initio* cluster calculations. Very importantly, this work shows that the magnetic orbital is essentially supported by the $3d_{xy}$ Cu orbital with a delocalization tail on the surrounding O $2p$ orbitals, the average repartition being 2/3 and 1/3, respectively. Such a magnetic contribution of the oxygen orbitals is the largest found in spin chains, at least 3 times larger than that in Li_2CuO_2,[71] and has important consequences on the neutron scattering experiments: (a) the magnetic form factor for the spin-spin correlation functions is going to be very anisotropic due to the planar geometry of the orbitals involved[88] and (b) the phase factors of Cu and O will produce interferences that result in a rather unusual **Q** dependence of the structure factor of excitations.

From the *ab initio* calculations,[87] magnetic electrons are broadly distributed within the cluster, which results in a large oxygen contribution. This result and the presence of a large anisotropy of the spin-spin correlation functions lead us to the conclusion that the spin-orbit interactions within this cluster are going to be significant, probably more important than in ferromagnetic $La_5Ca_9Cu_{24}O_{41}$.[73] The occurrence of an orbital moment within the cluster is certainly the signature of uncompensated currents, even in this restricted geometry of edge sharing CuO_2 chains.

B. Trivial chirality

The intrinsic helicity of the spin excitations can, under appropriate conditions of magnetic field, gives rise to a antisymmetric spin-spin correlation function or dynamical magnetochirality. This feature is considered in the neutron scattering equations and is a general property of any magnetic system. In this paper we have examined the influence of M_{ch} on the scattering cross section of the spin-singlet to spin-triplet transitions in a spin-1/2 dimer compound. When compared with the classical systems, the interest of this quantum spins systems is twofold: (a) Excitations are well defined at sufficiently low temperatures and appear at finite energy. (b) Due to the nature of the excitations, spin singlet-to–triplet–transitions can be easily calculated (see Table I) and results are rigorous and general to *any* $S=1/2$ system exhibiting this singlet-ground state.[89] Each component of the triplet is going to split following the Zeeman energy term, $\hbar\omega_{1,\bar{1}} = \hbar\omega_0 \mp g\mu_B H$. The components that are important for our purposes are the $|1\bar{1}\rangle$ and $|11\rangle$ ones, whereas the $|10\rangle$ is dispersionless and lacks further interest and, furthermore, is not visible in the experimental configuration $H\|\mathbf{Q}$. The number of components available for scattering studies in this configuration is thus reduced to 2. The most appealing result of our experiment is that if a polarized neutron beam is created, then the chiral term is going to act differently on each one of the components of the triplet depending upon the polarization of the incident beam. Following the results in Table I and in the Appendix , the component $|11\rangle$ appears in the σ^{+-} channel, the "+" sign meaning that the arrows of H, of **Q**, and of P_0 point towards the same direction. The other component $|1\bar{1}\rangle$ becomes enhanced by M_{ch} in the σ^{-+} channel. We want to stress that M_{ch} is entirely part of the scattering cross section of the magnetic excitations, as it is proved by the exact cancellation [except for terms of $O(M_{ch,\bar{1}}/\rho_F)$] of the scattering cross section in the corresponding channels shown in Fig. 9 and perfectly reproduced in the equations (see the Appendix).

Interestingly, the use of polarized neutrons allows one to single out each one of the components of the triplet, thus endorsing detail studies as a function of pressure, magnetic field, and temperature, separately. Indeed in spin-singlet ground-state compounds with spin gaps of the order of 10–40 meV, magnetic fields do not allow for a clear separation of each one of the components of the triplet beyond the energy resolution. As a result, a large peak is seen in the scattering experiments that can hardly be analyzed. By combining magnetic fields with neutron polarization analysis this difficulty can be easily overcome. A further application of our results is in detecting spin-only molecular crystal field excitation—i.e., *dimer* (multi-*mer*) physics hidden in the energy spectra of many antiferromagnetic compounds and probably at the origin of specific behavior such as heavy fermion, superconductivity, etc.

C. Nontrivial chirality

Throughout this work we have implicitly assumed that the chain sublattice of $Sr_{14}Cu_{24}O_{41}$ does not support nontrivial dynamical chirality. This may not be totally true if the hypothesis of the presence of ring exchange in the 90° Cu-O-Cu bonds is further confirmed.[54,55,83] As well known from spin-ladder systems, this ring exchange is produced by a cyclic four-spin exchange and gives rise to a very intricate phase diagram, which includes ground states with vector or scalar chirality. Despite their underlying interest, these phases have not been observed yet. The proposed ring exchange in the chain sublattice[54,55,83] is of a different nature and so is the analogous phase diagram, yet to be determined. This ring exchange may turn out to be enhanced as a result of the strong antiferromagnetic interactions that mediate the Cu-···-Cu superexchange making up the dimer in the chain sublattice, as pointed out by Gellé and Lepetit.[87]

Nevertheless, such a chiral interaction vector would be perpendicular to the plane of chains and will thus remain undetectable in our experiments. The nontrivial dynamic magnetochirality scattering cross section arises from the presence of an axial vector interaction and contains the projection of the spin-spin cross product, $\mathbf{C}=\mathbf{S}_i\times\mathbf{S}_j$, in the following form[21]:

$$M_{ch}^{C} \propto (\mathbf{P}\cdot\mathbf{C}). \tag{8}$$

Nontrivial dynamical magnetochiral fluctuations can be seen as *phason*-like (or twist) as well as *amplitudon*-like excitations of the helix (or variations of the pitch of the helix) or soliton-type Bloch domain walls.[23] Note that both types of fluctuations of the helix can be understood as equal and unequal variations of the phase between operators $\mathbf{S}_i$ and $\mathbf{S}_j$, respectively. Although not much is known about the properties of these modes in chiral magnetic systems, we expect

that both are low-lying energy modes. In our experiment, and because $\mathbf{P} \perp \mathbf{C}$, we do not expect any nontrivial dynamic magnetochirality contributions to appear in our neutron scattering experiments, if any.

A different proposal of nontrivial magnetochiral effects arises from *hidden* order parameters that embody electronic degrees of freedom in highly covalent molecules. We have seen in the Introduction that a number of proposals have appeared in the literature to explain particular features in high-T_C superconductors. Quantum spin ladders such as the ladder sublattice of $Sr_{14}Cu_{24}O_{41}$ have been seen to display features that can be interpreted as the effect of spin currents, ring exchange, biquadratic exchange, and four-spin exchange, all these terms being used in the literature to name the same effect.[90,91]

V. CONCLUSIONS

In this paper we have carried out a thorough neutron polarization analysis study of the quantum magnetic excitations in the spin-chain compound $Sr_{14}Cu_{24}O_{41}$. Two main results unfold from our study. First, the spin-spin correlation functions are found to be rather anisotropic whereas the spin triplet remains degenerate within our instrument resolution. Both features are hard to reconcile within the standard, but otherwise simple, picture of a magnetic interaction model. We speculate on the origin of this anisotropy as arising from orbital electronic currents that induce an effective orbital moment to the dimer. Finally, we have evidenced the presence of antisymmetric inelastic spin-spin correlation functions under an external magnetic field. The experimental conditions were exactly the same as those set up for chiral compounds. However, the material under consideration is a spin-liquid, paramagnetic compound that exhibits a spin-singlet ground state and the lattice structure supports an inversion center. P symmetry is, therefore, not violated in the ground state and, thus, this compound is not chiral. The presence of these antisymmetric inelastic spin-spin correlation functions is quantitatively accounted for under the basis of singlet-to-triplet molecular crystal field excitations. The fact that both trivial and nontrivial chirality shares analogous selection rules pleads against rapid conclusions in the polarized inelastic neutron scattering experiments under a parallel-to-**Q** magnetic field in paramagnetic compounds.

ACKNOWLEDGMENTS

We wish to acknowledge enlightening discussions with J. P. Boucher at the early stages of this work. O. Cepas and T. Ziman have also largely contributed to the understanding of the origin of the Dzyalozhinskii-Moriya antisymmetric interactions. The support of the ILL technical staff is greatly acknowledged.

APPENDIX

Here we calculate the cross sections taking into account Eqs. (1) and (2) and Table I. For the case $H \| P_0 \| \mathbf{Q}$, the convention goes as follows: $x \| Z$, $y \| \{X,Y\} \equiv v$ and $z \| \{X,Y\} \equiv w$, where v and w represent a linear combination of operators S_X and S_Y, with v and w orthogonal. The most obvious choice is $S_v \equiv S_X$ and $S_w \equiv S_Y$. We have dropped the nuclear correlation function that appears in the non-spin-flip channels, as it is irrelevant in this calculation. In order to account for the anisotropy of the correlation functions, two phenomenological parameters a and b are used in the calculations:

$$M_y(|11\rangle) = M_y(|1\bar{1}\rangle) \propto a^2(\hbar\omega)\langle S_v \cdot S_v^\dagger \rangle = a^2(\hbar\omega),$$

$$M_z(|11\rangle) = M_z(|1\bar{1}\rangle) \propto b^2(\hbar\omega)\langle S_w \cdot S_w^\dagger \rangle = b^2(\hbar\omega),$$

$$M_{ch}(|11\rangle) = -M_{ch}(|1\bar{1}\rangle) \propto iab(\langle S_v \cdot S_w^\dagger \rangle - \langle S_w \cdot S_v^\dagger \rangle)$$
$$= -2a(\hbar\omega)b(\hbar\omega), \tag{A1}$$

and $M_{11} \equiv M_y(|11\rangle) + M_z(|11\rangle)$ and $M_{1\bar{1}} \equiv M_y(|1\bar{1}\rangle) + M_z(|1\bar{1}\rangle)$. As each component of the triplet occurs at different energies (in the presence of a magnetic field) we further define $a_1 \equiv a(\hbar\omega_1)$, $b_1 \equiv b(\hbar\omega_1)$, $a_{\bar{1}} \equiv a(\hbar\omega_{\bar{1}})$, and $b_{\bar{1}} \equiv b(\hbar\omega_{\bar{1}})$, and $\hbar\omega_1 = \hbar\omega_0 - g\mu_B H$ and $\hbar\omega_{\bar{1}} = \hbar\omega_0 + g\mu_B H$. The scattering cross sections under polarized neutrons for $|11\rangle$ and $|1\bar{1}\rangle$ read as follows:

$$\sigma_x^{+-}(|11\rangle) \propto a_1^2 + b_1^2 + 2a_1 b_1,$$

$$\sigma_x^{-+}(|11\rangle) \propto a_1^2 + b_1^2 - 2a_1 b_1,$$

$$\sigma_x^{+-}(|1\bar{1}\rangle) \propto a_{\bar{1}}^2 + b_1^2 - 2a_{\bar{1}} b_{\bar{1}},$$

$$\sigma_x^{-+}(|1\bar{1}\rangle) \propto a_{\bar{1}}^2 + b_1^2 + 2a_{\bar{1}} b_{\bar{1}}. \tag{A2}$$

Taking into account the anisotropy $M_z/M_y = b_1^2/a_1^2 = b_2^2/a_2^2 \approx 1.4$, then it is straightforward to calculate the cross sections above:

$$\sigma_x^{+-} \propto a_1^2 + 0.007 a_{\bar{1}}^2,$$

$$\sigma_x^{-+} \propto 0.007 a_1^2 + a_{\bar{1}}^2. \tag{A3}$$

Note that the contribution of $a_{\bar{1}}$ (compared to that of a_1) in the $+-$ polarization channels is rather small (of the order of 0.7%) and it can be ignored. The opposite applies to a_1 in the $-+$ channels. This value of $a_{\bar{1}}$ in the $+-$ channel arises from the anisotropy of the spin-spin correlations between the z and y directions. Strictly speaking, these relations hold valid for an infinitly good neutron flipping ratio ($\rho_F \to \infty$). To account for the finite flipping ratio of the polarization analysis a term $M_{ch}/(1+\rho_F)$ has to be added to the equations above:

$$\sigma_x^{+-} \propto a_1^2 + 0.024 a_{\bar{1}}^2,$$

$$\sigma_x^{-+} \propto 0.024 a_1^2 + a_{\bar{1}}^2. \tag{A4}$$

As expected the amount from the finite flipping ratio is more important than that of the anisotropy. The contribution of $a_{\bar{1}}$

in the +− polarization channels is finally of the order of 2.4% for $\rho_F=30$ and can be safely neglected in our experiment. Therefore, and for many of the purposes in inelastic neutron scattering experiments, we can approximate the above equation by

$$\sigma_x^{+-} = M_{11} + M_{ch} + \overbrace{(M_{11}^{-} - M_{ch})}^{0},$$

$$\sigma_x^{-+} = \underbrace{(M_{11} - M_{ch})}_{0} + M_{11}^{-} + M_{ch}. \tag{A5}$$

[1] X. G. Wen, F. Wilczek, and A. Zee, Phys. Rev. B **39**, 11413 (1989).

[2] Y. Taguchi, Y. Oohara, H. Yoshizawa, N. Nagaosa, and Y. Tokura, Science **291**, 2573 (2001).

[3] T. Taniguchi, K. Yamanaka, H. Sumioka, T. Yamazaki, Y. Tabata, and S. Kawarazaki, Phys. Rev. Lett. **93**, 246605 (2004).

[4] For a recent review, see P. A. Lee, N. Nagaosa, and X.-G. Wen, Rev. Mod. Phys. **78**, 17 (2006).

[5] C. M. Varma, Phys. Rev. B **55**, 14554 (1997); Phys. Rev. Lett. **83**, 3538 (1999).

[6] Sudip Chakravarty, R. B. Laughlin, Dirk K. Morr, and Chetan Nayak, Phys. Rev. B **63**, 094503 (2001).

[7] A. Kaminski, S. Rosenkranz, H. M. Fretwell, J. C. Campuzano, Z. Li, H. Raffy, W. G. Cullen, H. You, C. G. Olson, C. M. Varma, and H. Höchst, Nature (London) **416**, 610 (2002).

[8] B. Fauque, Y. Sidis, V. Hinkov, S. Pailhes, C. T. Lin, X. Chaud, and Ph. Bourges, Phys. Rev. Lett. **96**, 197001 (2006).

[9] H. Kawamura, J. Phys.: Condens. Matter **10**, 4707 (1998).

[10] All these arguments can be identically applied to uniaxial ferromagnets, as well.

[11] The spin-waves equation of motion reads as follows:

$$\frac{d\vec{S}_n}{dt} = \vec{S}_n \times \vec{H}_n^{eff},$$

and $\vec{H}_n^{eff}$ is the effective magnetic field produced by the nearest-neighbor exchange interactions J and the (single ion in this case) anisotropy D,

$$\vec{H}_n^{eff} = -2J(\vec{S}_{n-1} - \vec{S}_{n+1}) + 2DS_n^z\vec{e}_z.$$

[12] Antiferromagnetic compounds do not macroscopically violate T symmetry as there are an equal number of spins ↑ than ↓.

[13] We have decided to use the word *trivial* dynamical magnetochirality to describe magnetic excitations that are not issued from a chiral ground state, although the understanding of this dynamical magnetochirality can be in some cases challenging and far from being trivial.

[14] M. Blume, Phys. Rev. **130**, 1670 (1963).

[15] S. V. Maleyev, V. G. Baryakhtar, and A. Suris, Sov. Phys. Solid State **4**, 2533 (1963).

[16] G. L. Squires, *Introduction to the Theory of Thermal Neutron Scattering* (Cambridge University Press, Cambridge, England, 1978), p. 152.

[17] S. W. Lovesey, *Theory of Neutron Scattering from Condensed Matter* (Oxford University Press, New York, 1984), Vol. 2. p. 172.

[18] V. Barzykin and L. P. Gor'kov, Phys. Rev. Lett. **70**, 2479 (1993).

[19] S. V. Maleyev, Phys. Rev. Lett. **75**, 4682 (1995).

[20] D. N. Aristov and S. V. Maleyev, Phys. Rev. B **62**, R751 (2000).

[21] S. V. Maleev, Phys. Usp. **45**, 569 (2002).

[22] S. V. Maleyev, Physica B **345**, 119 (2004); **350**, 26 (2004).

[23] H.-B. Braun, J. Kulda, B. Roessli, D. Visser, K. W. Krämer, H.-U. Güdel, and P. Böni, Nat. Phys. **1**, 159 (2005).

[24] This type of dynamic magnetochirality is termed *hidden* by the authors.

[25] H.-B. Braun and D. Loss, Phys. Rev. B **53**, 3237 (1996); S. Takagi and G. Tatara, *ibid.* **54**, 9920 (1996); J. Kyriakidis and D. Loss, *ibid.* **58**, 5568 (1998); B. A. Ivanov, A. K. Kolezhuk, and V. E. Kireev, *ibid.* **58**, 11514 (1998).

[26] T. Asano, H. Nojiri, Y. Inagaki, Y. Ajiro, L. P. Regnault, and J. P. Boucher, cond-mat/0201298 (unpublished).

[27] S. V. Maleyev, V. P. Plakhty, O. P. Smirnov, J. Wosnitza, D. Visser, R. K. Kremer, and J. Kulda, J. Phys.: Condens. Matter **10**, 951 (1998).

[28] V. P. Plakhty, S. V. Maleyev, J. Kulda, J. Wosnitza, D. Visser, and E. V. Moskvin, Europhys. Lett. **48**, 215 (1999).

[29] V. P. Plakhty, S. V. Maleyev, J. Kulda, E. D. Visser, J. Wosnitza, E. V. Moskvin, Th. Brückel, and R. K. Kremer, Physica B **297**, 60 (2001); V. P. Plakhty, W. Schweika, Th. Brückel, J. Kulda, S. V. Gavrilov, L. P. Regnault, and D. Visser, Phys. Rev. B **64**, 100402(R) (2001).

[30] B. Roessli, P. Böni, W. E. Fischer, and Y. Endoh, Phys. Rev. Lett. **88**, 237204 (2002).

[31] S. V. Grigoriev, S. V. Maleyev, A. I. Okorokov, Yu. O. Chetverikov, R. Georgii, P. Böni, D. Lamago, H. Eckerlebe, and K. Pranzas, Phys. Rev. B **72**, 134420 (2005).

[32] R. M. Moon, T. Riste, and W. C. Koehler, Phys. Rev. **181**, 920 (1969).

[33] L. P. Regnault (unpublished).

[34] P. J. Brown, J. B. Forsyth, and F. Tasset, Proc. R. Soc. London, Ser. A **442**, 1147 (1993).

[35] For a review, see Sander van Smaalen, Z. Kristallogr. **214**, 786 (1999).

[36] E. M. McCarron III, M. A. Subramaniam, J. C. Calabrese, and R. L. Harlow, Mater. Res. Bull. **23**, 1355 (1988).

[37] A. Frost-Jensen, V. Petrícek, F. Krebs Larsen, and E. M. McCarron III, Acta Crystallogr., Sect. B: Struct. Sci. **53**, 125 (1997).

[38] M. Uehara, T. Nagata, J. Akimitsu, H. Takahashi, N. Mori, and K. Kinoshita, J. Phys. Soc. Jpn. **65**, 2764 (1996).

[39] M. Isobe, T. Ohta, M. Onoda, F. Izumi, S. Nakano, J. Q. Li, Y. Matsui, E. Takayama-Muromachi, T. Matsumoto, and H. Hayakawa, Phys. Rev. B **57**, 613 (1998).

[40] M. Matsuda, K. Katsumata, H. Eisaki, N. Motoyama, S. Uchida, S. M. Shapiro, and G. Shirane, Phys. Rev. B **54**, 12199 (1996).

[41] L. P. Regnault, J. P. Boucher, H. Moudden, J. E. Lorenzo, A. Hiess, U. Ammerahl, G. Dhalenne, and A. Revcolevschi, Phys. Rev. B **59**, 1055 (1999).

[42] M. Matsuda, T. Yosihama, K. Kakurai, and G. Shirane, Phys. Rev.

B **59**, 1060 (1999).
[43] F. C. Zhang and T. M. Rice, Phys. Rev. B **37**, 3759 (1988).
[44] J. Etrillard, M. Braden, A. Gukasov, U. Ammerahl, and A. Revcolevschi, Physica C **403**, 290 (2004).
[45] M. Braden, J. Etrillard, A. Gukasov, U. Ammerahl, and A. Revcolevschi, Phys. Rev. B **69**, 214426 (2004).
[46] M. v. Zimmermann, J. Geck, S. Kiele, R. Klingeler, and B. Büchner, Phys. Rev. B **73**, 115121 (2006).
[47] P. Abbamonte, L. V. A. Rusydi, G. A. Sawatzky, G. Logvenov, and I. Bozovic, Science **297**, 581 (2002).
[48] P. Abbamonte, G. Blumberg, A. Rusydi, P. G. Evans, T. Siegrist, A. Gozar, H. Eisaki, E. D. Isaacs, and G. A. Sawatzky, Nature (London) **431**, 1078 (2004).
[49] A. Rusydi, P. Abbamonte, H. Eisaki, Y. Fujimaki, G. Blumberg, S. Uchida, and G. A. Sawatzky, cond-mat/0511524 (unpublished).
[50] A. Revcolevschi, A. Vietkine, and H. Moudden, Physica C **282-287**, 493 (1997); U. Ammerahl, G. Dhalenne, A. Revcolevschi, J. Berthon, and H. Moudden, J. Cryst. Growth **193**, 55 (1998); U. Ammerahl and A. Revcolevschi, *ibid.* **197**, 825 (1999).
[51] J. E. Lorenzo, L. P. Regnault, and C. Boullier (unpublished).
[52] C. Boullier, PhD thesis, Université Joseph Fourier, Grenoble, France, 2005.
[53] M. Matsuda and K. Katsumata, Phys. Rev. B **53**, 12201 (1996).
[54] V. Kataev, K.-Y. Choi, M. Grüninger, U. Ammerahl, B. Büchner, A. Freimuth, and A. Revcolevschi, Phys. Rev. Lett. **86**, 2882 (2001).
[55] V. Kataev, K.-Y. Choi, M. Grüninger, U. Ammerahl, B. Büchner, A. Freimuth, and A. Revcolevschi, Phys. Rev. B **64**, 104422 (2001).
[56] In antiferromagnetic compounds there is, by definition, an equal number of spins ↑ and spins ↓. In ferromagnets, the magnetic field favors a given orientation by shrinking the unfavorable domains which ends up in a single domain if the magnetic field strength can overcome the coercive field.
[57] M. Hase, I. Terasaki, and K. Uchinokura, Phys. Rev. Lett. **70**, 3651 (1993).
[58] M. Isobe and Y. Ueda, J. Phys. Soc. Jpn. **65**, 1178 (1996).
[59] H. Kageyama, K. Yoshimura, R. Stern, N. V. Mushnikov, K. Onizuka, M. Kato, K. Kosuge, C. P. Slichter, T. Goto, and Y. Ueda, Phys. Rev. Lett. **82**, 3168 (1999); H. Kageyama, J. Phys. Soc. Jpn. **69**, 65 (2000).
[60] P. R. Hammar and D. H. Reich, J. Appl. Phys. **79**, 5392 (1996).
[61] G. Chaboussant, P. A. Crowell, L. P. Lévy, O. Piovesana, A. Madouri, and D. Mailly, Phys. Rev. B **55**, 3046 (1997).
[62] D. C. Johnston, J. W. Johnson, D. P. Goshorn, and A. J. Jacobson, Phys. Rev. B **35**, 219 (1987).
[63] T. Barnes and J. Riera, Phys. Rev. B **50**, 6817 (1994).
[64] This experiment is not possible in the present compound as the scattering cross section is proportional to the Bose factor, which is very small at these energies and temperatures.
[65] S. W. Lovesey, *Theory of Neutron Scattering from Condensed Matter* (Oxford University Press, New York, 1984), Vol. 2, p. 183.
[66] T. Freltoft, G. Shirane, S. Mitsuda, J. P. Remeika, and A. S. Cooper, Phys. Rev. B **37**, 137 (1988);
[67] X. L. Wang, L. L. Miller, J. Ye, C. Stassis, B. N. Harmon, D. C. Johnston, A. J. Schultz, and C. Loong, J. Appl. Phys. **67**, 4524 (1990).
[68] S. Shamoto, M. Sato, J. M. Tranquada, B. J. Sternlieb, and G. Shirane, Phys. Rev. B **48**, 13817 (1993).
[69] Y. Sasago, K. Uchinokura, A. Zheludev, and G. Shirane, Phys. Rev. B **55**, 8357 (1997).
[70] F. Sapiña, J. Rodríguez-Carvajal, M. J. Sanchis, R. Ibañez, A. Beltran, and D. Beltran, Solid State Commun. **74**, 779 (1990).
[71] E. M. L. Chung, G. J. McIntyre, D. M. Paul, G. Balakrishnan, and M. R. Lees, Phys. Rev. B **68**, 144410 (2003).
[72] M. Boehm, S. Coad, B. Roessli, A. Zheludev, M. Zolliker, P. Boni, D. McK. Paul, H. Eisaki, N. Motoyama, and S. Uchida, Europhys. Lett. **43**, 77 (1998).
[73] M. Matsuda, K. M. Kojima, Y. J. Uemura, J. L. Zarestky, K. Nakajima, K. Kakurai, T. Yokoo, S. M. Shapiro, and G. Shirane, Phys. Rev. B **57**, 11467 (1998).
[74] T. Thio, T. R. Thurston, N. W. Preyer, P. J. Picone, M. A. Kastner, H. P. Jenssen, D. R. Gabbe, C. Y. Chen, R. J. Birgeneau, and A. Aharony, Phys. Rev. B **38**, 905 (1988); M. A. Kastner, R. J. Birgeneau, T. R. Thurston, P. J. Picone, H. P. Jenssen, D. R. Gabbe, M. Sato, K. Fukuda, S. Shamoto, Y. Endoh, K. Yamada, and G. Shirane, *ibid.* **38**, 6636 (1988).
[75] U. Ammerahl, B. Büchner, C. Kerpen, R. Gross, and A. Revcolevschi, Phys. Rev. B **62**, R3592 (2000).
[76] O. Cepas, K. Kakurai, L. P. Regnault, T. Ziman, J. P. Boucher, N. Aso, M. Nishi, H. Kageyama, and Y. Ueda, Phys. Rev. Lett. **87**, 167205 (2001).
[77] L. Shekhtman, O. Entin-Wohlman, and A. Aharony, Phys. Rev. Lett. **69**, 836 (1992).
[78] W. Koshibae, Y. Ohta, and S. Maekawa, Phys. Rev. Lett. **71**, 467 (1993).
[79] L. Shekhtman, O. Entin-Wohlman, and A. Aharony, Phys. Rev. Lett. **71**, 468 (1993).
[80] C. J. Peters, R. J. Birgeneau, M. A. Kastner, H. Yoshizawa, Y. Endoh, J. M. Tranquada, G. Shirane, Y. Hidaka, M. Oda, M. Suzuki, and T. Murakami, Phys. Rev. B **37**, 9761 (1988).
[81] T. Yildirim, A. B. Harris, A. Aharony, and O. Entin-Wohlman, Phys. Rev. B **52**, 10239 (1995).
[82] O. Entin-Wohlman, A. B. Harris, and Amnon Aharony, Phys. Rev. B **53**, 11661 (1996).
[83] Sabine Tornow, O. Entin-Wohlman, and Amnon Aharony, Phys. Rev. B **60**, 10206 (1999).
[84] H.-A. Krug von Nidda, L. E. Svistov, M. V. Eremin, R. M. Eremina, A. Loidl, V. Kataev, A. Validov, A. Prokofiev, and W. Assmus, Phys. Rev. B **65**, 134445 (2002).
[85] M. Matsuda, H. Yamaguchi, T. Ito, C. H. Lee, K. Oka, Y. Mizuno, T. Tohyama, S. Maekawa, and K. Kakurai, Phys. Rev. B **63**, 180403(R) (2001).
[86] M. Matsuda, K. Kakurai, S. Kurogi, K. Kudo, Y. Koike, H. Yamaguchi, T. Ito, and K. Oka, Phys. Rev. B **71**, 104414 (2005).
[87] A. Gellé and M.-B. Lepetit, Eur. Phys. J. B **46**, 489 (2005).
[88] The form factors for the Cu and the oxygen in the edge sharing configuration can be found in Ref. 69.
[89] Identical polarized neutron scattering experiments carried on another 1D spin chain compound, $CuGeO_3$, have shown identical results.
[90] Y. Honda, Y. Kuramoto, and T. Watanabe, Phys. Rev. B **47**, 11329 (1993).
[91] S. Brehmer, H. J. Mikeska, M. Muller, N. Nagaosa, and S. Uchida, Phys. Rev. B **60**, 329 (1999); A. Nakasu, K. Totsuka,

Y. Hasegawa, K. Okamoto, and T. Sakai, J. Phys.: Condens. Matter **13**, 7421 (2001); K. Hijii and K. Nomura, Phys. Rev. B **65**, 104413 (2002); T. S. Nunner, P. Brune, T. Kopp, M. Windt, and M. Grüninger, *ibid.* **66**, 180404(R) (2002); T. Hikihara, T. Momoi, and X. Hu, Phys. Rev. Lett. **90**, 087204 (2003); T. Momoi, T. Hikihara, M. Nakamura, and X. Hu, Phys. Rev. B **67**, 174410 (2003); A. Läuchli, G. Schmid, and M. Troyer, *ibid.* **67**, 100409 (2003); K. P. Schmidt, H. Monien, and G. S. Uhrig, *ibid.* **67**, 184413 (2003); K. Hijii, S. Qin, and K. Nomura, *ibid.* **68**, 134403 (2003); V. Gritsev, B. Normand, and D. Baeriswyl, *ibid.* **69**, 094431 (2004); B. Normand and A. M. Oleś, *ibid.* **70**, 134407 (2004).